Modeling the Impacts of Urbanization vs. Green House Gas Warming in Southern California Coasts

Bereket Lebassi[1] and Jorge E. Gonzáleze[2]*

[1]Department of Mechanical Engineering, Santa Clara University, Santa Clara, CA

[2]Mechanical Engineering Department, City College of New York, New York, NY

Robert Bornstein[3]

[3]Department of Meteorology, San José State University, San José, CA

****Corresponding author email: gonzalez@me.ccny.cuny.edu***

ABSTRACT

A recent study by Lebassi et al. 2008 evaluated long-term (1948-2005) air temperatures in California (CA) during summer (June-August, JJA). The aggregate CA results showed asymmetric warming, as daily minimum temperatures increased faster than daily maximum temperatures. The spatial distributions of daily maximum temperatures in the heavily urbanized South Coast (SoCAB) and San Francisco Bay Area (SFBA) air basins in California, however, exhibited a complex pattern, with cooling at low-elevation coastal-areas and warming at inland areas. Previous studies have suggested that cooling summer max temperatures in CA were due to increased irrigation, coastal upwelling, or cloud cover. The current hypothesis, however, is that this temperature pattern arises from a "reverse-reaction" to greenhouse gas (GHG) induced global-warming. In this hypothesis, the global warming of inland areas resulted in an increased (cooling) sea breeze activity in coastal areas.

Further investigation using mesoscale simulation (RAMS), with a horizontal grid resolution of 4 km on an innermost grid over SoCAB are undertaken to investigate the effect of urbanization on the coastal flow patterns and compared with the possible impacts of global warming. Results show that the effect of urbanization on coastal environment is twofold. The mechanical properties deter the sea breeze flows while the thermal aspect enhances the sea breeze. The comparison of present and past climate conditions reflect significant increase in sea breeze and coastal cooling which supports the hypothesis that coastal cooling is a possible direct result of global warming.

Significant societal impacts may result from this observed reverse-reaction to GHG-warming. Possible beneficial effects (especially during periods of UHI growth) include decreased maximum: O_3 levels, per-capita energy requirements for cooling, and human thermal-stress levels.

1. Introduction

Urban heat islands (UHI) have been extensively studied using observational data (e.g. Bornstein 1968; Price 1979; Rao 1972; Landsberg, 1981; Gallo et al., 1993; Tso, 1995; Jauregui and Romales, 1996; Jauregui, 1997; Lo et al. 1997; Brian 2000) and numerical simulations (e.g. Lebassi 2006, Myrup 1969; Dixon et al. 2003). UHIs represent a clear local indicator of land use induced climate change and their impacts are observed in urban/rural convective circulation patterns. These circulation contrasts are most significant during clear and calm conditions and

tend to disappear in cloudy and windy weather. Goodridge (1991) used 112 station average temperatures records to show the urban heating influences on long-term California air temperature trends. He analyzed 80-year 2m air temperature and showed that UHI effects influenced the magnitude of the observed warming trend in the overall data set. These warming trends also correspond to areas containing the State's major population centers, with observed warming magnitude increasing in counties with higher population. Cooling trends were also observed in rural areas and counties with small population size. Goodridge also showed that surface sea temperature (SST) warming was found to be highly correlated with the warming of 2m air temperature at coastal land observation stations.

In the current study we focus on the impacts of urbanization on coastal environment on the SoCAB region of California. This region is highly urbanized and populated where the importance of the research is large. The main objective of the present paper is to analyze the impacts on urbanization under a changing climate under the lights of our recent reported discovery for coastal cooling of this region. We attributed this finding to a reverse reaction of global warming. The approach utilized for the analysis is the use of validated mesoscale modelling for the region with improved land surface parameterization. An ensemble of four short-terms simulations is organized to explore the separate and combined effects of land use and global warming.

2. Methodology

2.1 Methodology Overview

The mesoscale model used is the Regional Atmospheric Simulation System (RAMS) model. This is a highly versatile non-hydrostatic numerical model developed at Colorado State University. It solves the Reynolds-averaged primitive equations, which are described by Tripoli and Cotton (1986). The model uses a quasi Boussinesq approximation, and "time-split" time differencing (Pielke 1984). RAMS uses the Arakawa C staggered grid in which thermodynamic and moisture variables are defined at the grid volume center, and velocity components are defined at half grid points (Mesinger and Arakawa 1976). A Polar stereographic map projection is used for the horizontal grid domain, and a terrain-following sigma coordinate system with variable grid spacing is used in the vertical in order to increase the resolution near the surface The RAMS model can be initialized as variable field model initialization, where the four dimensional data assimilation (4DDA) uses time series of gridded variables of horizontal wind, potential temperature, and relative humidity values that are analyzed from either observations or large-scale model forecasts (e.g. NCEP, ETA).

The ensemble of simulations consisted of four simulations that represented the present (2002), past (1970), and natural potential vegetation (NPV) each consisting of ten summer days. The present was taken as the periods 0000 UTC 01-10 June 2002 and 0000 UTC 01-10 August 2002. The past was taken as 0000 UTC 01-10 August1970 and 0000 UTC 01-10 June 2002 with a non-urbanized land use (PNV). The present was taken as the validation period. The combination of the simulations generated the following three cases; Present vs Observations; Present LCLU – PNV; Present-Past.

2.2 Model Setup

Two fixed nested grids, centered over the SoCAB, were employed in the study. The two innermost grids (20 and 4 km, respectively) are two-way interactive. The coarser grids will

simulate (Grid 1) synoptic conditions, while the innermost fine grid (Grid 2) will explicitly resolve deep moist convection and will have grid spacing of 4 km. There are 30 vertical layers, stretched from a spacing of 0.03 to 1.2 km in the first 7.5 km of the atmosphere and then maintained at a spacing of 1.2 km above that to the model top at 22 km.

The RAMS simulations focused on the analysis of the heat island in northern California Central Valley. For this purpose, a nested-grid configuration was implemented. The outer model domain was extended eastward to include most of the western United States, and westward a considerable distance seaward (Fig. 1). Finer nested grids were applied over the area of interest in order to obtain meteorological fields at higher resolutions.

Figure 1. Nested grid configuration of the modeled region. (grid 1: red, grid 2: green, grid 3: blue, grid 4: black)

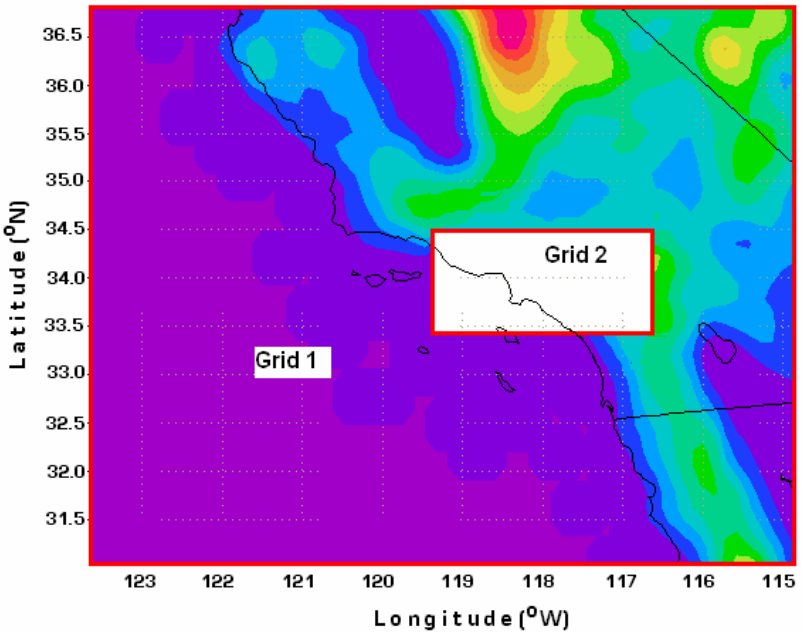

Two nested grids were chosen to select important physical features of the meteorology. The domain for the outer grid was set to be large enough to capture the synoptic high pressure systems important for the simulation cases. The second grid was chosen to resolve the details of the coastal mountains and inland effects. The detailed configuration that was selected and applied to the specified periods of simulation is described in the next section.

2.3 Case Description and Input data

Our two case studies are designed to examine relevant unsolved problems. Previous observational research has been able to detect a heating trend of the Northern (and inland) Central Valley cities (Lebassi et. al. 2005) in the case of summertime months of June, July and August (JJA). A follow up observational study (Lebassi et al. 2008) indicated that coastal cooling and inland warming was observed in the SoCAB and attributed to global warming. RAMS will be used to answer the outstanding questions about the impacts of urbanization in SoCAB and particularly on the sea breeze from the coastal areas of Southern California, under changing climate. This region has bays with a non-linear coastline and complex inland

topography that can influence both the sea breeze and the UHI. An ensemble consisting of ten days simulation periods for the present, past, and PNV were chosen summer months. The first land use scenario was configured considering the current land cover and land use (LCLU) of SoCAB hereafter referred as *case 1* (Fig. 2).

Figure 2. LULC map for case 1 (19, 22, 24 are urban, 12 is shurabland)

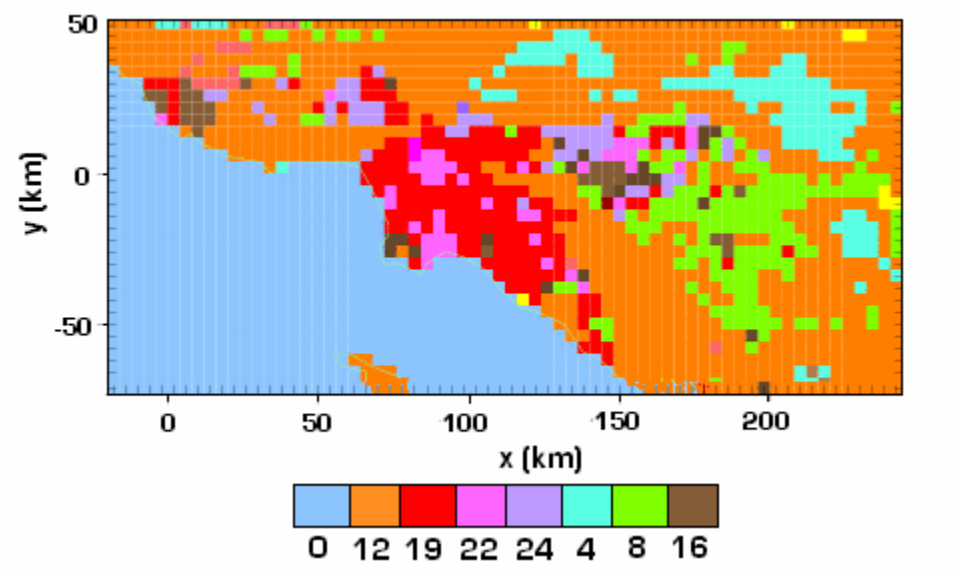

As part of the model configuration, the current (2002) CA LCLU representation in RAMS was undertaken. A methodology was developed to incorporate LCLU data derived from NOAA 30m resolution 38 urban class LCLU to the modified regional model. Higher resolution LCLU is necessary to resolve the complex subgrid scale phenomenon, which will produce a more detailed analysis of the various atmospheric fields. LEAF-3 is a surface–vegetation–atmosphere transfer (SVAT) model that currently contains 21 land surface types, most of which are defined in BATS (Dickinson et al. 1986). For this research study 3 urban classes (Residential, Commercial and Rural) were added expanding the total LEAF-3 classes to 24. Within any grid cell, multiple patches (7 used for this research) can be used to represent the heterogeneity of vegetation classes. For urban land types, leaf area index and vegetation fractional coverage are minimized, and roughness length is increased to approximate the effects of barren rough city surfaces. For the region of interest there are only three major urban LCLU classes, which dominate the region. These are the residential, commercial building and rural classes. These classes were added in the LEAF-3 submodel and the 8 physical and thermal parameters associated with these classes were carefully defined based on literature and data on SoCAB. One of the important parameters to be determined was the urban vegetation fraction. A technique was developed to determine the urban vegetation fraction from high resolution Google™ earth visible images. The following procedures where used to calculate the urban vegetation fraction.

- Start with visible Google map (Fig. 3 left panel)
- Change map to only 16 colors (Fig. 3 center panel)
- Count pixel values in selected typical area for each urban class
- Calculate fractions of green colors to determine vegetation fraction
- Change map to only 2 colors (black & white) (Fig. 3 right panel)

- Count black and white pixels
- Calculate fractions of white colors to determine rooftop fractions
- Street fractions are the black fraction minus the vegetation fraction
- Only vegetation fractions for each urban class can be input in current RAMS lookup table.

Figure 3. Google earth high resolution images for urban vegetation calculations (left, raw image, center 16 color, and right 2 color)

The second simulation case modified the urban land use structure of the SoCAB to reflect the pre-urbanization, hereafter referred as *case 2*. The only change made in *case 2* from *case 1* was modification of the urban LCLU to shrub land (class 12) which is the dominant land use class in the region. As a result all the physical and thermal properties of the urban were changed to that of shrub land in case 2.

The other important consideration in studying dense urban arrears is anthropogenic heat sources. Anthropogenic heating in typical US cities is estimated as 60% due to traffic, 40% due to residential and industrial activities and few percentages due to human metabolism (Sailor and Lu 2004). Previous researches had considered a constant anthropogenic heat addition in their urban related studies (Saito et al. 1995). In this research we implemented a variable daily profile of anthropogenic heat from data reported by Sailor and Lu (2004) (Fig. 4).

Figure 4. Anthropogenic heat profiles

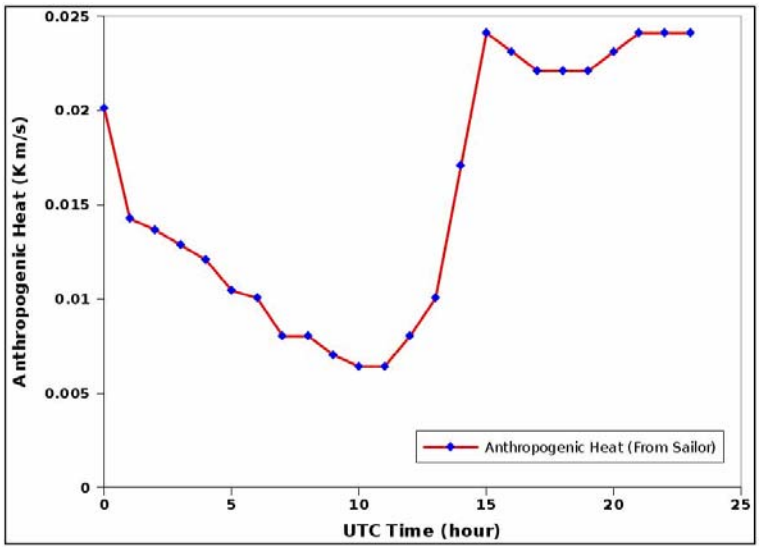

Data source (Sailor and Lu 2004)

The variable anthropogenic heat was implemented at the subgrid level where it was added to surface heat fluxes for each urban subgrid patch. Figure 4 shows a morning and after noon pick associated with the morning and afternoon traffic rush hours.

2.4 Initialization

Initialization of the RAMS simulations requires four types of input data: (1) topographic data that characterizes the elevation of the land surfaces; (2) sea surface temperature data that provides the temperature of the sea surface over the Pacific Ocean; (3) vegetation data that characterizes land surface characteristics; and (4) meteorological data that characterizes meteorological fields at the initial time, at the boundaries, and at synoptic distance scales. We describe each of these inputs here.

- Topography files: The USGS topography data set of 1 km resolution was used.
- SST files: The sea surface temperature (SST) data set from RAMS consists of mean climatologically monthly values with a resolution of 1 degree (about 100 km).
- Vegetation files: The 30m NOAA vegetation, which is mentioned above is used.
- Meteorological fields: The model was initialized with gridded data sets prepared by the isentropic analysis package embedded in RAMS. The primary meteorological data was retrieved from the National Center for Environmental Prediction (NCEP). Their horizontal increment is 0.5 degree, and data are available every 6 hours (0000, 0600, 1200 and 1800 UTC). The lateral boundary conditions on the outer grid followed the Klemp-Lilly condition, which is a variant of the Orlanski condition (Klemp et. al. 1978). Here, gravity wave propagation speeds computed for each model cell are averaged vertically, with the single average value being applied over the entire vertical column. The horizontal diffusion coefficients were computed as the product of the horizontal deformation rate and a length scale squared, based on the original Smagorinsky (1963) formulation. The vertical diffusion coefficients were computed according to the Mellor and Yamada (1974) parameterization scheme, which employs a prognostic turbulent kinetic energy variable. For both shortwave and long wave radiation parameterizations, the scheme described by Mahrer and Pielke (1977) has been used.
- The roughness length is defined according to the vegetation cover.
- Water balance: The simulation also allowed for the condensation of water vapor to cloud water, and the microphysical parameterization of any species of liquid or ice. The mean rain, snow, aggregate, graupel or hail droplet diameter was specified from the default value in the RAMS code. The number concentration is diagnosed automatically from this mean diameter and the forecast mixing ratio.

3. Results

3.1 Model Validation

In order to have confidence in the simulations, a validation of the model results against available observations was carried out. For the specified simulation period, the model reproduced the synoptic scale forcing, namely the locations of the high and low pressure systems very well. To gain insight into how well the model simulation depicted the thermal forcing of the low-level flow, the model surface temperature and wind speed fields were also compared to

observations. Time series of surface temperature (hereafter temperature) of 12 stations at the SoCAB were averaged and examined. These stations were representative covering inland and coastal areas which are shown in Figure 5.

Figure 5. SoCAB METR Observational Stations

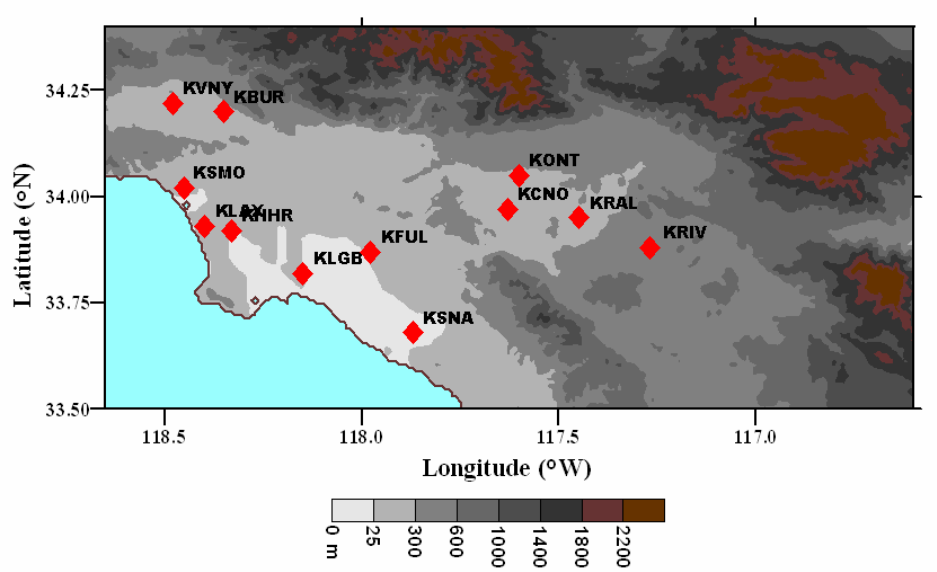

Model vs. observation surface 2m temperature comparisons for the 12 stations averaged is shown in Figure 6a. It can be noted that the model compares very well with the observations capturing the day to day variation of surface temperature. It has captured the average cooling trend in the first three days followed by four warm days and then another three day cooling trend. The model captured the day and night temperature except some discrepancies on the maximums of the three warm days (Fig. 6a). The ten day average observed temperatures was 19 ^{o}C, while the model showed 20 ^{o}C. Similar comparisons where also performed for the 10m wind speeds of the 12 SoCAB stations.

Figure 6a Model vs. Observation 2m temperature comparisons

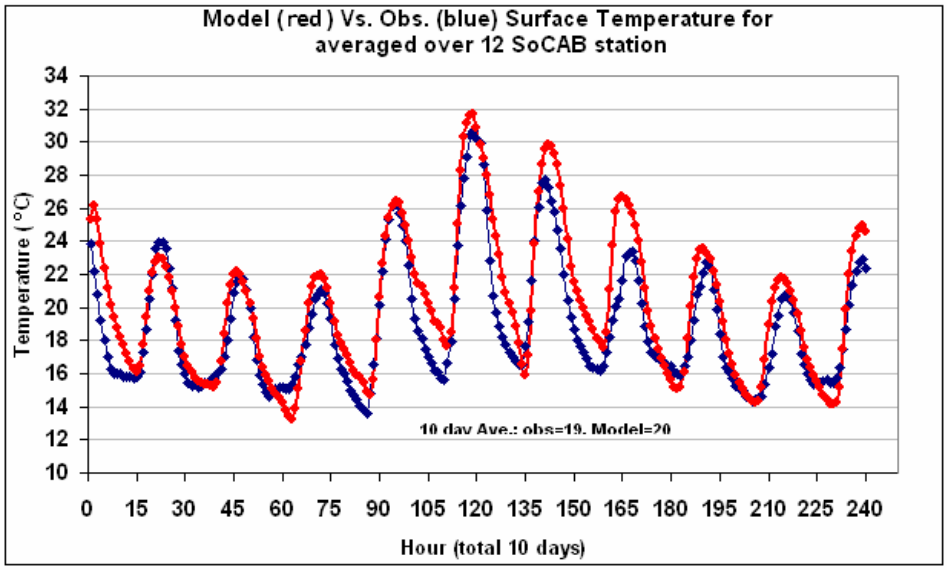

The Average 10m wind speed is shown on Figure 6b. Again, the model compares very well with the observations capturing the maximum, minimum and daily variations of the wind speed. There are minor discrepancies on few days at night when the wind is calm. The ten day average wind speed for both the model and observations are calculated to be exactly 3 m/s.

Figure 6b Model vs. Observation 10m wind speed comparisons

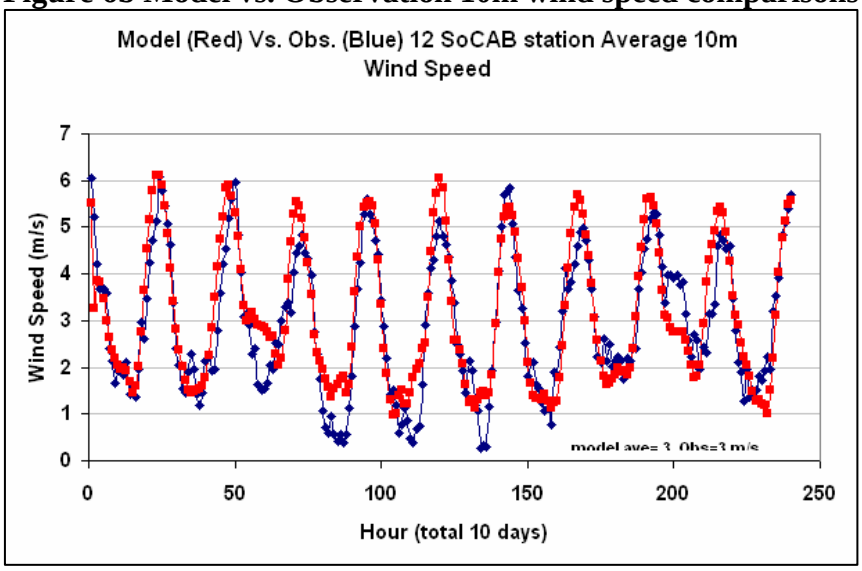

3.2 Observational result

The present study focuses on the connection urbanization in inducing coastal cooling. Daytime summer coastal cooling in coastal urban areas implies that UHI warming was weaker than the reverse-reaction sea breeze cooling; with possibilities of larger sea breeze cooling in the absence of UHI. Analysis of daytime summer max temperatures at four adjacent pairs of urban and rural sites near the inland cooling-warming boundary, however, showed that the rural sites experienced cooling, while the urban sites showed warming due to UHI development. The rate of heat island growth was estimated as the sum of each urban warming rate and the absolute magnitude of the concurrent adjacent rural cooling rate. The effects of growing UHIs on T_{max}

trends were analyzed by use of four close-by urban and rural station-pairs: Stockton and Sacramento in the SFBA and Pasadena and Santa Ana in the SoCAB. Results (Fig. 7) showed a UHI of 0.55, 0.51, 0.26, and 0.12^{o}C decade^{-1} respectively, and were proportional to changes in urban population and horizontal area.

The urban centers in SoCAB have grown tremendously in terms of population and area. Part of their observed increased JJA T_{max}-values could be attributed to increased daytime UHI-intensity. Without UHI effects, the currently observed JJA SFBA coastal-cooling area might have expanded to include these sites, as the first three are adjacent to rural airport sites that showed cooling T_{max}-values due to increased marine influences. In addition, all urbanized sites with decreasing T_{max}-values would probably show even larger cooling rates if UHI effects could be removed.

Figure 7. Summer 1970-2005 2m Tmax trends for four urban-rural pairs: (a) Stockton, (b) Sacramento, (c) Pasadena, and (d) Santa Ana; where solid trend lines (blue points) and dashed trend lines (red points) represent the rural and urban sites, respectively.

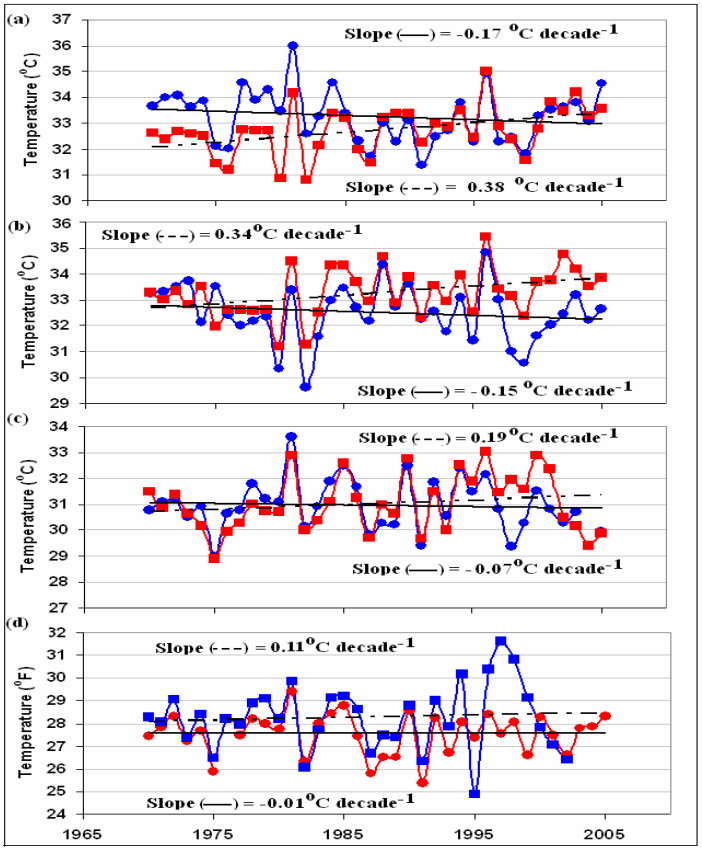

b. Preliminary Modeling Result

To investigate the marine flow patterns and variations in flow intensity as function of land use, simulations with the Regional Atmospheric Modeling System RAMS (version 6.0) were performed. Two cases were chosen varying the land cover of the SoCAB. The first land cover scenario was done for the current land cover hereafter called Present. The second case simulation was a reconstruction of the land cover, which removes the urban centers in the SoCAB, hereafter will be called as PNV.

RAMS simulations were executed to improve the understanding of the flow patterns in the SoCAB Bay Basin and the investigation of possible changes in coastal flow intensities as function of land cover. The ten-day average wind vector difference combined with the average difference in temperatures for the two cases were investigated.

Results are shown for the high resolution grid (grid 2) in the next 3 figures. Figure 8 shows the ten days average 8 LST temperature difference and the wind vector difference plotted over it. There is a difference temperature of 2 ^{o}C over most of the urban regions of the SoCAB. At this time the sea breeze have yet to start while the land breeze was still there. The difference wind vectors show that there is stronger land breeze (1 m/s increases) resulting from the heat island in the present than in the past. As a result the heating has advected towards the coast significantly.

Figure 8. Present-PNV temperature and wind vectors average over the 8 AM LST of ten days (temperatures in ^{o}C, wind in m/s)

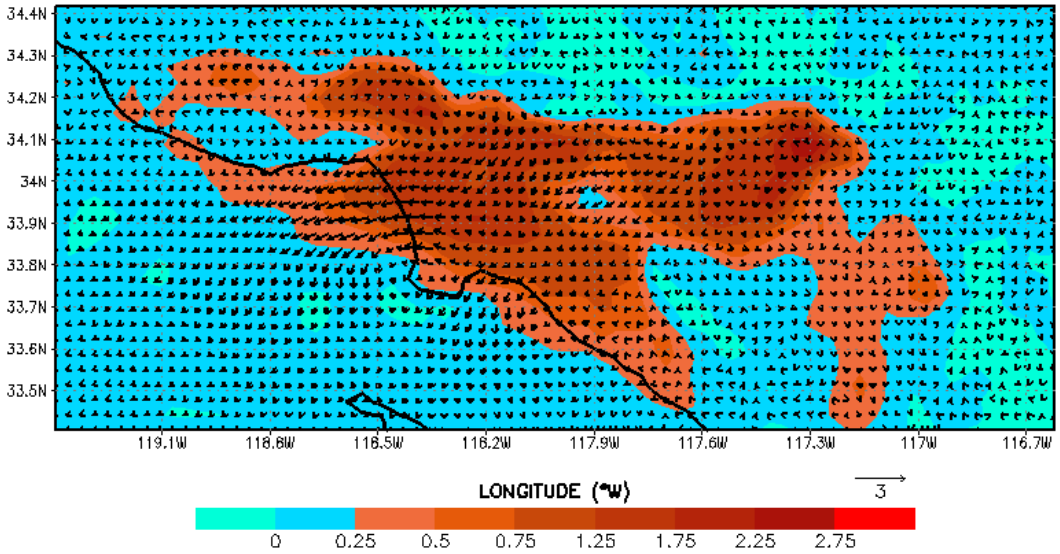

However, during the day where the sea breeze had fully developed, the mechanical aspect has stronger impact than the thermal aspect of the land use change. Figure 9 shows the difference in surface temperatures and wind vectors between the present and PNV at 2 PM LST. Smaller differences in temperature of 1 ^{o}C are observed over the coast as compared to the difference mentioned above. The heat had also shrank its extent, while the difference in wind vectors show that the wind speed in the present decreased over the urban region by 2 m/s as compared to PNV. This is do to the roughness increases in the urban regions due to built up the city was compared to then non-built up PNV.

Figure 9. Present-PNV temperature and wind vectors average over the 2 PM LST of ten days (temperatures in ^{o}C, wind vector decrease in m/s)

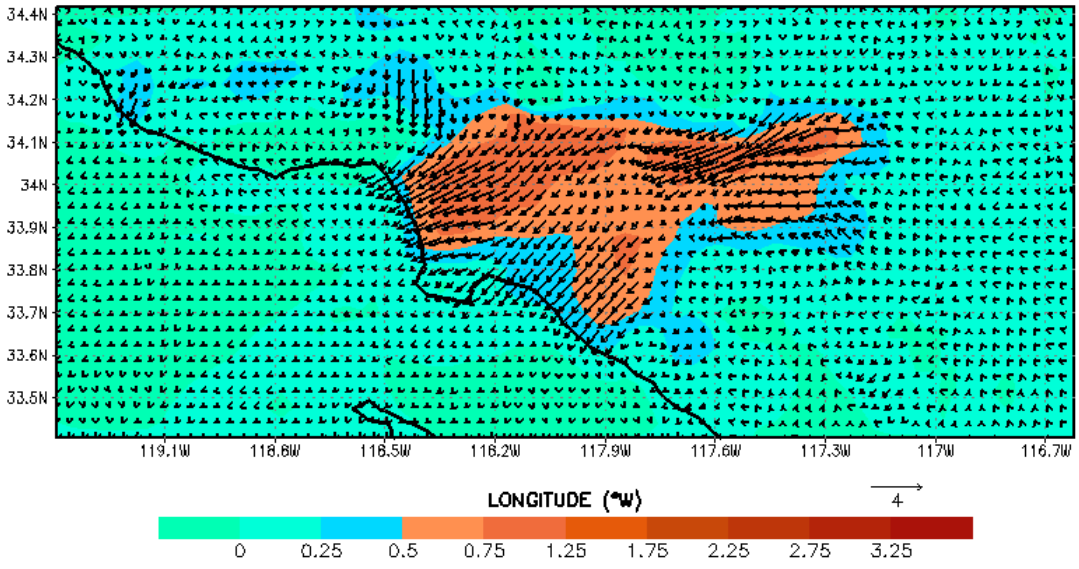

The effect of the urbanization on vertical extent is also shown in Figure 10. The cross section is at 34 ^{o}N latitude. The effect over the built up is shown up to 500 m where temperature difference are shown up to 2.75 ^{o}C at the surface and 1 ^{o}C aloft.

Figure 10. Present-PNV 8 AM LST vertical temperature profile averaged over ten days cross section at 34 ^{o}N latitude (temperatures in ^{o}C)

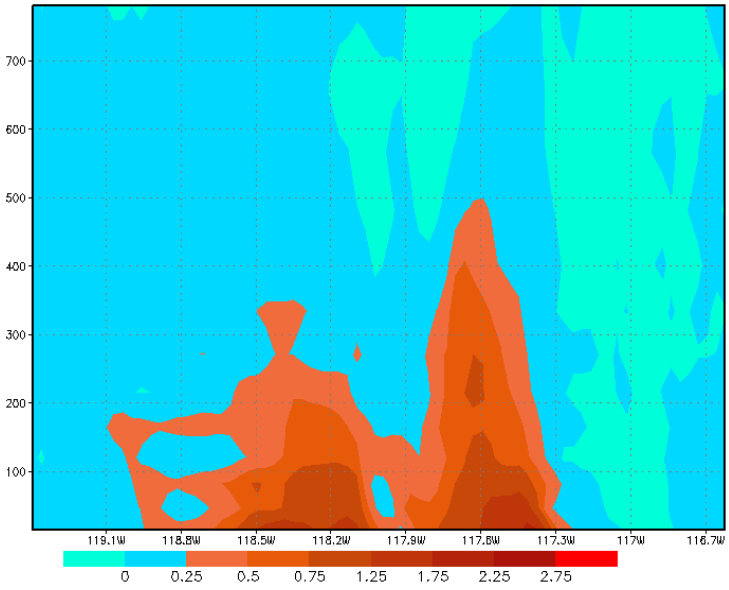

For the June 2002 simulation of past and present cases the heat Island growth was observed while the flow was deterred over the city. To study the possible impact of climate change a similar case study of the warmest month of August was undertaken, referred as *case 3*. For this past simulation, 1970 August (1-10), was taken as past reference case, while the present case was taken as for August (1-10) of 2002, referred as *case 4*. The atmospheric conditions and the sea surface temperatures were changed to their respective years and days to reflect changes in global climate, while the land use change was assumed to be small.

Figure 11. Present-Past (1970) 4 PM LST temp. and wind vectors (temp. in ^{o}C, wind m/s)

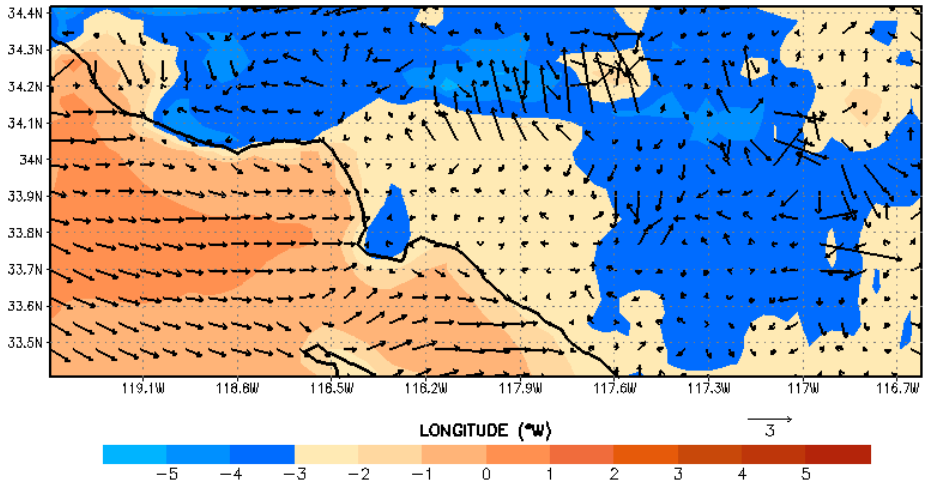

The result is presented in Figure 11, and it shows very interesting findings. The figure shows the 4 Pm LST difference temperature and wind vector fields averaged over the 10 days period simulation. There is a clear acceleration of the flow (2-3 m/s) over the ocean and decrease in the temperatures over the land. While the degree of the temperature changes differs with less decreases over the city, inland and higher elevations and more decrease on non-urban and low elevations. This is a promising preliminary result that supports coastal cooling. More analysis and longer period of simulations will be undertaken in the near future to further sustain these claims.

4. Conclusion

Results of four simulation cases were presented in this paper to further investigate changes in regional climate in SoCAB. The simulations attempted to quantify the impacts of LCLU and of global changing climate. The ensemble consisted of four present LCLU scenarios (June & August 2002), the potential natural LCLU scenario, and reconstruction of past climate conditions. Comparison of the observation vs. model temperature and winds showed a very promising agreement. This is due to the inclusion of high resolution LCLU, inclusion of subgrid effects and anthropogenic heating. Results for impacts of LCLU (Present-PNV) indicated that a ten days averaged morning and afternoon temperature differences of 1-2.75 ^{o}C results which enhance the land breeze by 1-2 m/s and deterred the sea breeze over the built up by 1-2 m/s during the day. This is due to the roughness of the city dominating the thermal effects during the day while the roughness of the built up did not have an impact on the land breeze. This is only urbanization impacts observed. Simulations to explore the impacts of global climate change since 1970 indicated that cooling trends are observed with increased flow patterns over the ocean. This validates the previous results observational study by the group of authors which that hypothesized that local sea breeze may increase as a reverse reaction of global warming.

5. References

Brian Pon, Dan Moses Stamper-Kurn, Craig Kenton Smith, and Hashem Akbari, 2000. *"Existing climate data sources and their use in heat island research"* (Tech. Rep. LBL-41973, Orlando Lawrence Berkeley National Laboratory, California, 2000).

Bornstein, R. D., 1968. *Observations of the urban heat island effect in New York City*. J Appl. Meteor., 7, pp. 575-582.

Cressie, N. A. C., 1991. *Statistics for Spatial Data*, John Wiley and Sons, Inc., New York.

Dixon, P. G., and Mote, L. T., 2003. *Patterns and causes of Atlanta's urban heat island-initiated precipitation*, J. Appl. Meteor., 42, pp. 1273-1284.

Dickinson, R. E., P. J. Kennedy, and M. F. Wilson, 1986. *Biosphere–Atmosphere Transfer Scheme (BATS) for the NCAR Community Climate Model*. NCAR Tech. Note NCAR/TN275+STR, 69 pp. [Available from National Center for Atmospheric Research, Boulder, CO 80307.]

Jauregui, E., 1997. *Heat island development in Mexico City*. J. Atmos. Env., 31B, pp. 3821-3831. Jauregui, E., and Romales, E., 1996. Urban effects of Convective Precipitation in Mexico City. J. Atmos. Env., 30B, pp. 3383-3389.

Gallo, K. P., A. L. McNab, T. R. Karl, J. F. Brown, J. J. Hood, and J. D. Tarpley, 1993. *The use of a vegetation index for assessment of the urban heat island effect, International Journal of Remote Sensing*, 14, 11, 2223-2230, 1993.

Goodridge, J. D., 1991. *Urban bias influence on long-term California air temperature trends*, J. Atmos. Env., 26B, pp. 1-7.

Klemp, J.B. and D.K. Lilly, 1978. *Numerical simulation of hydrostatic mountain waves*. J. Atmos. Sci.,35, 78-107.

Landsberg, H. E., 1970. *Man-made climate changes. Science*, 170, pp. 1265-1274.

Lebassi, B., J. JE. Gonzalez, D. Fabris, E. P. Maurer, N. Miller, C. Milesi, P. Switzer and R. Bornstein, 2008: *Observed 1970-2005 cooling of summer daytime temperature in coastal California.* J. Climate (inpress)

Lebassi B. H, J. E. González, D. Fabris, N. L. Miller, and C. Milesi, 2006. *Modeling urban heat islands in California Central Valley, Preprints of the AMS 6th Symposium on the Urban Environment*, Paper 3.1. Atlanta, GA.

Lebassi B., D. Fabris, J. E. Gonzalez, S. Zarantonello, S. Chiappari, N. L. Miller, and R. Bornstein, 2005. U*rban heat islands in California's Central Valley*, AMS BAMS, November 2005, pp. 1542-1543.

Lo, C. P.; Quattrochi D. A. and Luvall, J. C., 1997. *Applications of high-resolution thermal infrared remote sensing and GIS to asses the urban heat island effect. International Journal of Remote sensing*, 18, No. 2, pp. 287-204.

Lyons, W. A., Pielke, R. A., Tremback, C. J, Walko, R. L., Moon, D.A., Keen, C.S., 1995. *Modeling impacts of messocale vertical motions upon coastal zone air pollution dispersion, Atmospheric Environment*, 29, pp. 283-301.

Mahrer, Y., and R. A. Pielke, 1977. *The effect of topography on sea and land breezes in a two dimensional numerical model.* Mon. Wea. Rev., 105, 115–1162.

Mellor, G., and T. Yamada, 1974. *A hierarchy of turbulence closure models for planetary boundary layer.* J. Atmos. Sci., 31, 1791-1808.

Mesinger, F. and A. Arakawa, 1976. *Numerical methods used in atmospheric models*. GARP Publication Series, No. 14, WMO/ICSU Joint Organizing committee, 64 pp.

Myrup, L. D., 1969. *A numerical model of the urban heat island*. J. Appl Meteor., 16, 11-19. Price, J. C., 1979: Assessment of the urban heat island effect through the use of satellite data. Mon. Wea. Rev., 107, pp. 1554-1557.

Pielke, R. A., 1984. *Mesoscale Meteorological Modeling*. Academic Press, CA 612 pp.

Pielke, R. A., 1974. *A three-dimensional numerical model of the sea bree-ze over south Florida*. Mon. Wea. Rev., 102, 115–139.

Rao, P.K. 1972. *Remote sensing of urban heat islands from an environmental satellite*. Bull. Amer. Meteor. Soc., 53, pp. 647-648.

Saitoh T S, Shimada T, Hoshi H, 1995. Modeling and simulation of the Tokyo urban heat island. *Atmospheric Environment*, 30, 3431–3442.

Sailor D J, Lu L, 2004. A top-down methodology for developing diurnal and seasonal anthropogenic heating profiles for urban areas. *Atmospheric Environment*, 38, 2737–2748.

Smagorinsky, J., 1963. *General circulation experiment with the primitive equations. Part I, The basic experiment*. Mon. Wea. Rev., 91, 99-164.

Tripoli, G. J., Cotton W. R., 1982. *The Colorado State University three-dimentional cloud/mesoscale model – 1982. Part I: General theoretical framework and sensitivity experiments*. J. de Rech. Atmos., 16, 185-220.

Tso, C. P., 1995. *A survey of urban heat island studies in two tropical cities*. J. Atmos. Env., 30, pp. 507-519.

US Department of Transportation, Highway administration: http://www.fhwa.dot.gov/ohim/hs00/hm72 Desert Research Institute, Reno Nevada: http://www.wrcc.dri.edu/cgibin/cliMAIN.pl?casacc+nca.htm.